The physical mechanism of ultra-fast flame acceleration

Vitaly V. Bychkov[1], **Damir M. Valiev**[1], **Lars-Erik Eriksson**[2]

[1]Institute of Physics, Umeå University, SE–901 87, Umeå, Sweden

[2]Department of Applied Mechanics, Chalmers University of Technology, SE-412 96 Gothenburg, Sweden

1 Introduction

A deflagration-to-detonation transition (DDT) is the one of the most intriguing and the least understood effects in hydrodynamics, combustion science, nonlinear physics and astrophysics. It is the key point in many technological applications like design of pulse-detonation engines of next generation aircrafts. Spontaneous flame acceleration is the most important stage of the DDT. Flame acceleration in channels has been attributed qualitatively by Shelkin to wall-friction and turbulence [1]. Turbulence is a fatal obstacle for quantitative understanding and predicting the DDT, since turbulence and turbulent burning is a field of modern physics, which is far from being fully understood yet. To achieve powerful flame acceleration, modern experiments use obstacles in the channels. Optimal obstacle design was actively debated on the 21st ICDERS, Poitiers, France, 2007 [2, 3, 4]. Unfortunately, at present obstacle design employs mostly a painful "cut-and-try" approach with minor theoretical understanding. It relies mostly on the qualitative Shelkin mechanism, with the general belief that the main role of the obstacles is only to create stronger turbulence.

In the recent paper [5] we showed that the mechanism of ultra-fast flame acceleration in obstructed channels has the physical nature, which is qualitatively different from the Shelkin explanation. We found that delayed burning between the obstacles creates a powerful jet-flow driving the acceleration. The acceleration mechanism is independent of the Reynolds number, with turbulence playing only a supplementary role. The described mechanism is much closer in physical nature to initial acceleration of "tulip" flames explained by Clanet and Searby [6]. However, "tulip" flames accelerate only during a very short time, while the present mechanism works until detonation is triggered. We validate our theory by extensive numerical simulations and comparison to previous experiments. Here we report our results.

2 Formulation and analytical results

Similar to modern experiments [2, 3, 7, 8], in paper [5] we consider a channel of half-width R closed at one end, see Fig. 1. The channel is partly blocked by obstacles of height αR with free central part of half-width $(1-\alpha)R$. To elucidate the physical mechanism of flame acceleration, we start with tightly placed thin obstacles with spacing $\Delta z \ll \alpha R$. In this limit turbulence may be neglected; laminar burning goes slowly in the pockets between the obstacles with normal velocity U_f. Burning matter expands by the factor $\Theta = \rho_f/\rho_b$ determined by the density ratio of the fresh and burnt gas; the expansion factor is

Correspondence to : vitaliy.bychkov@physics.umu.se

typically $\Theta = 5-8$. Burnt gas flows out of the pockets with the speed $|u_x| = (\Theta-1)U_f$. Coming into the free channel part, the flow changes direction to the axial one, accumulates into a strong jet and pushes the leading flame tip forward. Flame sweeps extremely fast along the free channel part leaving behind new pockets of the fresh fuel mixture. This produces a positive feedback between the flame and the flow and leads to strong exponential acceleration of the flame tip. At the beginning, the flame velocity is low and the flow may be considered incompressible, $\nabla \cdot \mathbf{u} = 0$. Taking into account that $u_z = 0$ at the closed end $z = 0$, we find the velocity distribution in the free part of the channel with $|x| < (1-\alpha)R$

$$(u_x; u_z) = \frac{(\Theta-1)U_f}{(1-\alpha)R}(-x; z). \tag{1}$$

The flow becomes quite strong at large distances from the tube end, $z/(1-\alpha)R \gg 1$, when a large number of pockets contributes to the jet. The equation for the flame tip Z_f takes into account both the jet-flow and intrinsic flame propagation with velocity ΘU_f with respect to the burnt matter

$$\frac{dZ_f}{dt} = u_z(Z_f) + \Theta U_f = \frac{(\Theta-1)U_f}{(1-\alpha)R} Z_f + \Theta U_f. \tag{2}$$

Solution to Eq. (2) describes powerful flame acceleration

$$\frac{Z_f}{(1-\alpha)R} = \frac{\Theta}{\Theta-1}\left[\exp\left(\sigma U_f t/R\right) - 1\right] \tag{3}$$

with the scaled acceleration rate $\sigma = (\Theta-1)/(1-\alpha)$ independent of the Reynolds number. This mechanism is much stronger than the classical Shelkin mechanism, which becomes extremely weak in smooth tubes at large values of the Reynolds number, see the quantitative theory [9]. On the contrary, the present mechanism works even in very wide obstructed tubes with ideally slip walls. Acceleration becomes stronger for larger thermal expansion Θ and larger blockage ratio α. Wall-friction and turbulence play only supplementary roles in this mechanism, modifying burning between the obstacles. Flame propagation in the pockets between obstacles supports the jet in the free part of the channel and the exponential acceleration of the flame tip until detonation is triggered.

3 Simulation results

We validated the analytical theory by direct numerical simulations of the two-dimensional Navier-Stokes equations for a compressible reactive flow. The simulations are performed in the same way as in our recent papers [9]. The homogeneous gas mixture obeys the ideal gas law $P = (1-1/\gamma)\rho C_P T$, where $C_P = 10^3 \mathrm{m^2 s^{-2} K^{-1}}$ is the specific heat at constant pressure and $\gamma = 1.4$ is the adiabatic index. Initial temperature and pressure are $T_f = 300\mathrm{K}$, $P_f = 10^5\mathrm{Pa}$. We used the free-slip and adiabatic boundary conditions at the walls and obstacle surfaces. The channel half-width was $R = 24L_f$, where $L_f = \mu_f/\mathrm{Pr}\rho_f U_f$ is the so-called flame thickness, $\mu_f = 1.7 \cdot 10^{-5}\mathrm{kgs^{-1}m^{-1}}$ is the viscosity coefficient of fuel mixture and the Prandtl number is $\mathrm{Pr} = 0.75$. We took the initial Mach number within the range of $\mathrm{M} = U_f/c_s = 10^{-3} - 10^{-2}$. The lower value of the Mach number $\mathrm{M} = 10^{-3}$ corresponds to realistic methane and propane flames. We model reaction rate by a single-step Arrhenius kinetics. The scaled activation energy was $E/R_p T_f = 32$, where R_p is the ideal gas constant. The reaction rate is assumed to be of the first order. We took the Lewis number $\mathrm{Le} = 1$. We used the expansion factors $\Theta = 5, 8$, three values of the blockage ratio ($\alpha = 1/3; 1/2; 2/3$) and four values of spacing between the obstacles ($\Delta z/R = 1/4; 1/2; 1; 2$). The code is based on the cell-centered finite-volume method [10]. The numerical method has proved to be both accurate and robust for modeling of different kinds of complex reacting flows. The code has been validated by solving various hydrodynamic problems [10], and was utilized successfully in simulations of laminar flames at different conditions of burning [9]. Characteristic snapshots of the flame, the flow velocity and vorticity are shown in Fig. 1. Figs. 1 (a-c)

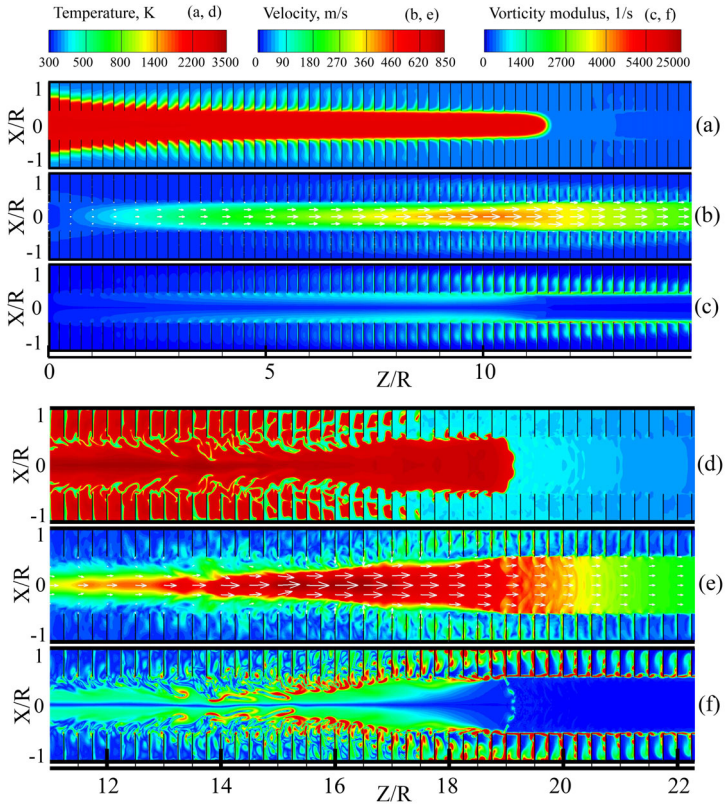

Figure 1: Snapshots of temperature, velocity and vorticity in the flow generated by an accelerating flame for $\Theta = 8$, $\mathrm{M} = 0.001$, $\Delta z/R = 1/4$, $\alpha = 2/3$ (a-c) and $\alpha = 1/2$ (d-f). Figure appears in [5].

reproduce the theoretical limit in the best way with the realistically small initial Mach number and tightly placed obstacles. In agreement with the above theory, the strongly accelerating flame front is confined in the free part of the channel; burning in the pockets is delayed. The gas flow shows a strong jet in the free channel part with practically no turbulence. Figs. 1 (d-f) show the flame front at the stage of developed acceleration, when the front propagation speed is comparable to the sound speed. Here the central jet generates quite strong turbulence, which makes the flame shape corrugated with much faster turbulent burning in the pockets. Still, the mechanism of flame acceleration described above keeps working not only qualitatively, but quantitatively even for strongly corrugated turbulent flames. Fig. 2 shows the position of the flame tip versus time and the tip velocity versus its position. We can observe the simulation results with different parameters coming in groups (shown by different colours). Orange markers in Fig. 2 (left) correspond to the same simulation parameters as in Fig. 1 ($\mathrm{M} = 10^{-3}$, $\Theta = 8$). They reproduce the incompressible limit in the best way and show very good agreement with the theory. Large values of the Mach number are beyond our incompressible model. To explore the model limitations, we also performed simulations with large initial values of the Mach number. We observe noticeably slower exponential flame acceleration at larger values of the Mach number; the deviation between the theory and modeling happens as the local Mach number comes close to one.

Figure 2 (right) compares the theory and simulations to the experiments by Johansen and Ciccarelli [3, 7], which are of the most recent and elaborated ones with the experimental setup geometry in line with the present theory and modeling. Johansen and Ciccarelli [3, 7] used obstacles with rather large spacing, which led to strong pulsations of the flame velocity due to flow contraction and expansion through the obstacle. Our theoretical model does not reproduce pulsations. Still, in average, the experiments, theory

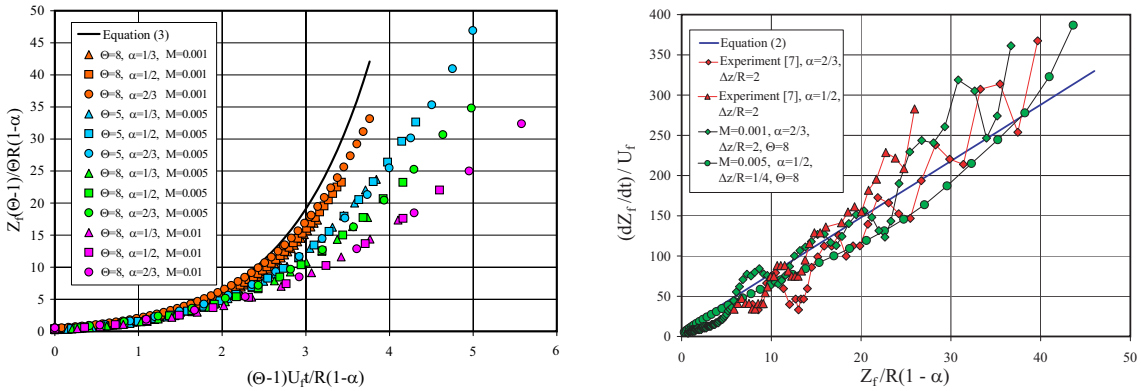

Figure 2: *Left:* Scaled position of the flame tip versus scaled time. Analytical solution (3) is shown by the solid line; numerical results are shown by markers. $\Theta = 5, 8$, $M = 0.001; 0.005; 0.01$, $\alpha = 1/3; 1/2; 2/3$. *Right:* Scaled velocity of the flame tip versus the scaled tip position. Red markers show experimental results of Ref. [3], solid straight line corresponds to the analytical solution (2), green markers show results of numerical modeling. Figure appears in [5].

and modeling are in a good agreement. Similar to the experiments, we performed several simulation runs with large spacing between the obstacles $\Delta z/R = 2$. Large spacing made the flame less confined, but it also led to stronger pulsations of the flame velocity similar to the experiments [3, 7]. Changing spacing of the obstacles, we obtained only minor changes in the average flame speed with the above theory working quite well. The explosion and detonation triggering is the final stage of DDT, which was also observed in the simulations and which will be presented in detail elsewhere.

The present theory and modeling reveal the physical mechanism of ultra-fast flame acceleration observed in modern experiments on detonation triggering. Understanding of this physical mechanism gives the capability for better control of the flame acceleration and DDT timing in different applications.

We thank Gaby Ciccarelli and Craig Johansen for the experimental data of Refs. [3, 7]. The work was supported by the Swedish Research Foundation and by the Kempe Foundation.

References

[1] Shelkin K. (1940). J. Exp. Teor. Phys. 10: 823

[2] Frolov S, Semenov I, Utkin P, Komissarov P, Markov V. (2007). Proceedings of 21st ICDERS, paper 215, Poitiers, France

[3] Johansen C, Ciccarelli G. (2007). Proceedings of 21st ICDERS, paper 242, Poitiers, France

[4] Gamezo V, Ogawa T, Oran E. (2007). Proceedings of 21st ICDERS, paper 114, Poitiers, France

[5] Bychkov V, Valiev D, Eriksson LE. (2008). Physical Mechanism of Ultra-Fast Flame Acceleration, Phys. Rev. Lett. 101, 164501

[6] Clanet C, Searby G. (1996). Combust. Flame 105: 225

[7] Johansen CT, Ciccarelli G. (2009). Combust. Flame 156: 405

[8] Kuznetsov M, Alekseev V, Matsukov I, Dorofeev S. (2005). Shock Waves 14: 205

[9] Bychkov V, Petchenko A, Akkerman V, Eriksson LE. (2005). Phys. Rev. E 72, 046307

[10] Wollblad C, Davidsson L, Eriksson LE. (2006). AIAA J. 44: 2340